DELFT UNIVERSITY OF TECHNOLOGY

DEPARTMENT OF AEROSPACE ENGINEERING

Report LR-301

KALMAN FILTER ORBIT IMPROVEMENT FROM KOOTWIJK LASER RANGE OBSERVATIONS

by

K.F. Wakker
B.A.C. Ambrosius
J.J.P. van Hulzen

Revised version of a paper presented at the 23rd COSPAR Meeting, Budapest, June 1980

DELFT - THE NETHERLANDS

September 1980

DELFT UNIVERSITY OF TECHNOLOGY

DEPARTMENT OF AEROSPACE ENGINEERING

Report LR-301

KALMAN FILTER ORBIT IMPROVEMENT FROM KOOTWIJK LASER RANGE OBSERVATIONS

by

K.F. Wakker
B.A.C. Ambrosius
J.J.P. van Hulzen

Revised version of a paper presented at the 23rd COSPAR Meeting, Budapest, June 1980

DELFT - THE NETHERLANDS

September 1980

Summary

Modern satellite ranging lasers emit short pulses at a low beam divergence and therefore require accurate satellite position predictions. This study aims at investigating the possibilities to use the laser range observations acquired at only one groundstation to provide real-time position prediction updates during each pass, and also better predictions for subsequent passes over that groundstation. A computer program, called SORKA, has been developed which is based on a sequential extended Kalman filter scheme. The objectives were to keep the program relatively simple to be compatible with small local computers, while still meeting the required accuracy level.

This report describes in some detail the computational approach adopted in SORKA. In particular, the methods to compute the state-transition matrix and the state-noise covariance matrix are emphasized. The dependence of the Kalman gain matrix on the reference state is shown and the techniques used in SORKA to improve the stability of the filter and to detect divergence are discussed. Some preliminary results using laser data acquired during 8 passes of GEOS-1 over the Kootwijk groundstation (The Netherlands) are presented.

Contents

1. Introduction

Since August 1976 the Department of Geodesy of Delft University of Technology operates a satellite laser ranging system at Kootwijk in the Netherlands. From there, the Working Group for Satellite Geodesy (WSG) acquires on a routine basis day and night ranging data for the geodetic satellites STARLETTE and GEOS-3, and only at night for LAGEOS. The ruby pulse-laser system consists of a multi-mode Q-switched oscillator, a spark-gap activated pulse chopper and two amplifier stages (Ref. 1, 2). The output energy in routine operation is 1 to 2 J, with a maximum of 3 J. The transmitted laser beam has a diameter of 19 cm and the divergence is adjustable from 1' to 20'. Until summer 1980, the system produced 4 ns wide pulses at a maximum rate of 15 pulses per minute. The measurements have shown an accuracy level of about 25 cm root-mean-square. Recently, a new chopper has been installed with a pulse-width of 2 ns, and a new range-gate generator having a manually adjustable time window with a minimum half-width of 0.1 μs. The latter facility would possibly give the capability of ranging to LAGEOS in daytime.

For many years there exists a close cooperation between WSG and the Section Orbital Mechanics (SOM) of the Department of Aerospace Engineering of Delft University of Technology. This Section supports WSG in the field of orbit computations for the geodetic satellites used in the laser ranging activities. This support ranges from satellite position predictions, needed for the automatic pointing of the laser, to orbit determination from laser observations acquired at Kootwijk and other laser ranging stations.

Within the period 1976 to 1979 more than 49,500 observations were obtained at Kootwijk during 1108 passes of BEACON-C, GEOS-1, GEOS-2, GEOS-3, SEASAT, STARLETTE and LAGEOS (Ref. 2). In 1979 alone, more than 20,000 observations were acquired during 369 satellite passes. It was found that quite often the actual satellite position deviated

so much from its predicted position that the laser pulse would have missed the satellite if the laser system would have operated in a fully-automatic blind-firing mode. To increase the accuracy of the laser pointings, it was decided in 1978 to investigate the possibilities to use laser observations from Kootwijk in a (semi-) real-time mode. This report describes part of the preliminary results of that study.

2. Laser pointing predictions

For the routine operations of pointing the laser at the satellite, at present use is made of the AIMLASER computer program, developed at the Smithsonian Astrophysical Observatory (SAO). This program has been modified by SOM to satisfy the specific needs of WSG and is regularly improved and updated. This Delft-version of AIMLASER (Ref. 3) is also in use at a number of other European laser stations. The input for the orbit prediction program consists of a set of mean orbital elements, distributed weekly by SAO. These parameters are determined by SAO from the so-called quick-look laser ranging data as returned to SAO by many ground-stations distributed all over the world.
Experience has shown that quite often the satellite position predictions on basis of these SAO elements and using the AIMLASER program reach a level of inaccuracy which is not compatible with lasers emitting a low-divergence beam. To give an indication of the accuracy needed, consider a satellite which passes over Kootwijk at a distance of 1000 km. When the beam divergence is 2', the diameter of the beam at the altitude of the satellite is 580 m. So, in this case a position prediction accuracy of about 500 m is needed in order to guarantee that the satellite is hit by the laser pulse.

To correct for position prediction errors, the Kootwijk laser system has been equipped with a manually controlable firing-time adjustment switch. During nighttime passes, if the satellite is sunlit, the operator may look through the laser telescope in order to estimate by what amount the firing time has to be delayed or advanced. This is possible for

satellites up to a visual magnitude of +13. Usually, however, if at the beginning of a pass no return signal is received, a systematic variation of the time adjustment is applied until returns are being registered. Sometimes, the adjustment can remain constant during a pass, but on other occasions re-adjustments are necessary. By this technique, the operator in fact corrects for position errors in the direction of the satellite's path across the sky. As an example, Fig. 1 shows the number of laser pulses, n, within intervals of 40 s during a pass of GEOS-3 and STARLETTE over Kootwijk on January 18 and Septem-

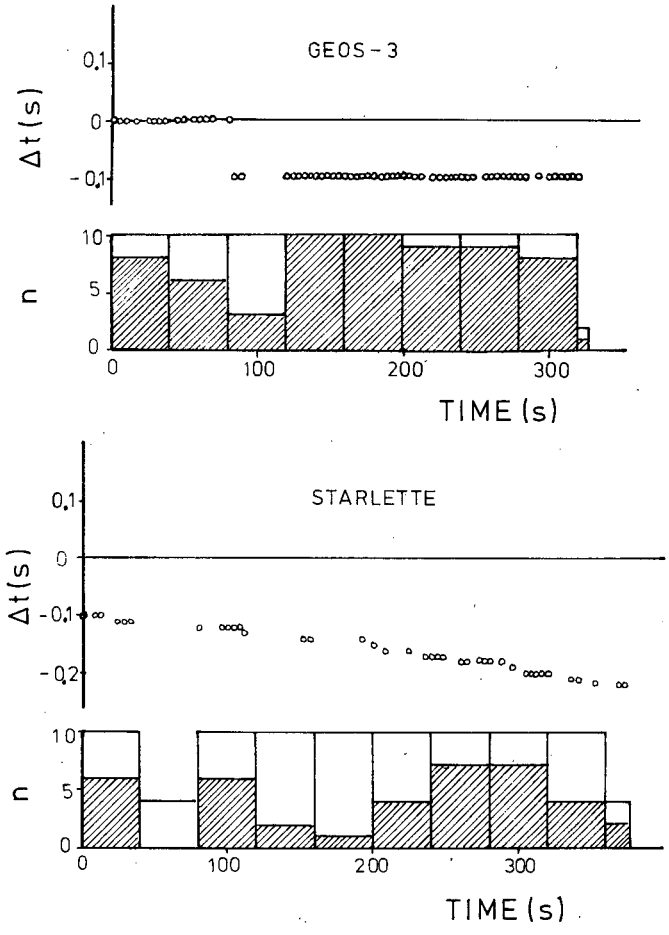

Fig. 1: The effect of the laser firing-time correction on the number of laser returns.

ber 14, 1977, respectively (Ref. 4). The laser operated at a rate of 15 pulses per minute and with a beam divergence of 3.5'. The shaded areas indicate the number of laser returns during each 40 s interval. Also shown is the time correction, Δt, applied by the operator. Clearly visible is the improvement obtained by the manual control of the laser firing-time.

One of the main disadvantages of this technique is that it corrects for in-track position errors only, while errors perpendicular to the satellite's path cannot be corrected for. It actually has occurred that the observer saw through the telescope that the satellite was too far from the predicted track without being able to apply corrections. Therefore, a need exists for more precise position predictions. This need becomes even more stringent with the development of more-advanced laser systems operating with a smaller beam divergence. But there is still another need for more accurate predictions.
To minimize the chances of false triggerings by noise pulses, a laser system uses a range-gate generator, which determines the time window in which the return signal is expected. For daytime ranging to distant satellites, like LAGEOS, very short windows of up to 0.1 μs are required. But this implies that the radial distance to the satellite has to be predicted with an accuracy of better than 30 m.

To increase the accuracy of the predicted satellite positions a number of possibilities exists. For instance, it would be possible to replace the SAO elements by more accurate orbital parameters and to use a satellite position prediction program that is more accurate than AIMLASER. In that case, laser observations from a number of groundstations are used to determine the orbit of the satellite very accurately. From this orbit determination an extremely accurate orbit is extrapolated for a long time in advance to yield one or more state vectors for each day. From these state vectors, the station generates its own laser pointing angles and computes the satellite's distance by numerical integration of the equations of motion. At Kootwijk, research is going on along

this line to improve the predictions for LAGEOS. It is doubtful, however, if such a technique will yield prediction accuracies for satellites below 1500 km altitude that satisfy the needs of the narrow-beam laser stations. Therefore, it is felt that it would be attractive to process in real time the laser range measurements registered during a pass over Kootwijk in order to increase the accuracy of the next laser pointings and window settings during that pass. This means that all computations have to be performed on an on-line computer within the period between two successive laser firings. The range measurements can also be used, however, in an off-line mode to improve the orbit for the next pass over Kootwijk. This also makes the station less dependent on a distant large computing center. This aspect could be of great importance for the mobile laser ranging systems now under development. These systems, however, are designed around low-power lasers (about 10 mJ per shot) operating with a beam divergence of about 0.5' and a high repetition rate of about 10 pulses per second. For these systems, signal levels are on the average below one photoelectron per shot for LAGEOS and in the order of ten photoelectrons per shot for satellites in lower orbits. As a result, large numbers of false returns are recorded which need to be identified in order not to upset the real-time orbit improvement scheme. Whether this is possible will not be discussed in this report, but a separate study on this subject is planned.

The main objective against the real-time laser pointing update approach is the fact that from the orbital mechanics point of view, it is very precarious to use range measurements from only one groundstation to improve the satellite's orbit. It is evident that from such observations during one pass very little information is gained on the orientation of the orbital plane. Therefore, the basic scheme presently envisaged is that range measurements obtained during several passes over Kootwijk yield the orientation of the orbit to such a level of accuracy that during the next pass the range measurements can be used in real time mainly to improve the prediction of the satellite's

position in the orbital plane. During the very first part of a pass some satellite searching process may be required. In that phase, the laser mount's angular position read-outs can possibly also be used as observation quantities. Though these angles will, in general, contain systematic errors, the inclusion of these quantities for the whole tracking period as quasi-observations with a relatively low weight might also be attractive to stabilize the orbit improvement process. Nevertheless, it is anticipated that, periodically, after long observation gaps, additional orbital information will be required which is derived from tracking data acquired at other groundstations.

3. The extended Kalman filter

It is well known that, basically, there exist two methods for processing satellite tracking data to estimate the orbit of a satellite. The batch processor, which yields the estimate at some reference epoch, requires that the entire sequence of observations be processed before the estimate can be made. On the other hand, the sequential orbit determination procedure processes one observation at a time and produces an estimate of the state vector at the observation time. So, this sequential procedure suits best the requirements for real-time orbit improvement, although it can also be used to predict the next satellite pass over the station. While the formal mathematical equivalence between the sequential estimation algorithm and the batch estimation algorithm can be shown, it is known from practical experience that the sequential process is much more sensitive to errors introduced by linearizations of the non-linear equations of motion and the observation-state relationships. These errors may result in estimate divergence problems.

The technique selected in this study is the extended Kalman filter, which is described in many textbooks (e.g. Ref. 5). An interesting geometric derivation of the Kalman filter equations is given in Ref. 6. Applications of the extended Kalman filter to orbit dynamics problems are discussed extensively in Refs. 7-12. For this study a computer program, called SORKA (Satellite Orbit Refinement using a KAlman filter)

has been developed, which at the moment functions primarily as a test program. It contains different options and alternatives to investigate in detail the Kalman filter characteristics for this application. It is emphasized here that the aim of SORKA is not to reach the high accuracy level and the extensive capabilities of computer programs like GEODYN or UTOPIA, but merely to satisfy the accuracy level needed for laser pointings and to be compatible with small local computers. To elucidate the description of the computational approach adopted in SORKA, a brief outline of the filter scheme will be given.

The satellite motion can be described by the set of equations

$$\dot{\underline{X}} = F\ (\underline{X},\ t)\ ;\ \underline{X}(t_0) = \underline{X}_0 \qquad (1)$$

where $\underline{X}$ denotes the state vector. When $\underline{X}_0$ is specified and F is known, the orbit of the satellite, and thus its state at a later time t_1, can be obtained from integration of Eq.(1). In orbit determinations, $\underline{X}_0$ is not known perfectly and therefore observations of the motion must be processed to obtain a more-accurate estimate for the state vector. Assume that a best estimate $\hat{\underline{X}}_0$ of the state at t_0 is known with an accuracy represented by the covariance matrix $\hat{P}_0$. Integration of Eq.(1) yields an initial state estimate at the time of the first observation t_1 : $\underline{X}_1$. Its covariance matrix, P_1, is computed from

$$P_1 = \phi_{1,0}\ \hat{P}_0\ \ \phi_{1,0}^T + Q_{1,0}$$

where $\phi_{1,0}$ is the state-transition matrix, used to map the state from t_0 to t_1 and defined by

$$\phi_{1,0} = \left(\frac{\partial \underline{X}_1}{\partial \underline{X}_0}\right)_{\hat{\underline{X}}_0}$$

and $Q_{1,0}$ is the state-noise covariance matrix, representing errors occurring during the state vector integration. These errors, which are assumed in this study to be Gaussian distributed with a zero mean,

include such effects as deterministic model errors, numerical integration errors and random process noise. The way this matrix is chosen will be discussed in Section 5.

The computation of $\underline{X}_1$ and P_1 from $\hat{\underline{X}}_0$ and $\hat{P}_0$ is called the time-update step. In the subsequent observation-update step the Kalman filter adds the information of the observations $\underline{Z}_1$ at t_1 to the initial estimates, yielding more-accurate estimates $\hat{\underline{X}}_1$ and $\hat{P}_1$. For this, in SORKA the general non-linear relations between the measured quantities and the state vector are used:

$$\underline{Z} = G\ (\underline{X},\ t) + \underline{V} \qquad (2)$$

where the stochastic vector $\underline{V}$ represents Gaussian distributed measurement errors with a zero mean and a covariance matrix R. The observation residuals at t_1: $\underline{z}_1$, are defined by

$$\underline{z}_1 = \underline{Z}_1 - \underline{Z}_1^*$$

where $\underline{Z}_1^*$ denotes the predicted observations as computed from Eq.(2) and the initial estimate $\underline{X}_1$:

$$\underline{Z}_1^* = G\ (\underline{X}_1,\ t_1)$$

The new estimate $\hat{\underline{X}}_1$ is given by

$$\hat{\underline{X}}_1 = \underline{X}_1 + K_1\ \underline{z}_1$$

where K_1 is a weight matrix. This matrix has to be chosen such that the new state estimate is optimal in some sense. A minimum-variance state estimate is obtained if K_1 is chosen to be the Kalman gain matrix, satisfying:

$$K_1 = P_1 H_1^T (H_1 P_1 H_1^T + R_1)^{-1} \qquad (3)$$

where H_1 is the observation matrix, defined by

$$H_1 = \left(\frac{\partial G}{\partial \underline{X}}\right)_{\underline{X}_1}$$

So, the matrix H is evaluated for the most accurate state estimate available at this stage: the reference state $\underline{X}_1$. The state covariance matrix at t_1 corresponding to the optimal state estimate can be found from

$$\hat{P}_1 = (I - K_1 H_1) P_1$$

where I is a unit matrix of appropriate dimensions. Once $\hat{\underline{X}}_1$ and $\hat{P}_1$ are known, the same process is repeated to compute the state and the state covariance matrix at the time of the next observation. In this way, the best estimate at any time contains the information of the last and all previous observations. It should be realized that the Kalman filter was developed for linear systems. Because the equations encountered in orbit dynamics are highly non-linear, appropriate linearizations had to be introduced. These lead to errors, which, as will be shown in Section 6, may cause serious problems.

The scheme given above holds for all types of observations. In this study, the observations are ranges from the laser to the satellite, but SORKA has been designed such that in the future also azimuth and elevation observations can be dealt with. As a reasonable assumption, range, azimuth and elevation can be considered independent observations. Then, a computational simplification is possible by permitting the individual observations at each observation time to enter the algorithm one after another as scalars. In that case, the term in brackets in Eq.(3) reduces to a scalar. So, the inversion of this term reduces to a division by a scalar, which avoids possible numerical pro-

blems occurring in matrix inversions.

For each time-update step, the function F, the state-transition matrix, ϕ, and the state-noise covariance matrix, Q, have to be evaluated. For the integration of the state equations, Eq.(1), a relatively simple force field has been assumed, accounting only for the first five zonal harmonics (J_2 to J_6) and the first tesseral harmonic ($J_{2,2}$) of the geopotential. For the required partial derivatives $\partial U/\partial \underline{X}$, where U represents the geopotential, analytical expressions have been derived (Section 4). The dynamical equations are integrated with a fourth-order Runge-Kutta method. The stepsize depends on the time between subsequent measurements and has an upper limit of 40 s. The computation of the state-transition matrix and the state-noise covariance matrix is described in the next Sections.

In each observation-update step, the function G and the matrices R and H are required. The measurement-noise covariance matrix is assigned the values of the known measurement noise variances. The observation matrix is evaluated at a reference state, usually taken as $\underline{X}_1$. In Section 6 an alternative for this reference state will be introduced.

4. The state-transition matrix

From Eq.(1) a differential equation can be derived for the state-transition matrix:

$$\dot{\phi}_{t,0} = \left(\frac{\partial F}{\partial \underline{X}}\right)_{\underline{X}_t} \phi_{t,0} \quad ; \phi_{0,0} = I \tag{4}$$

These so-called variational equations can be integrated numerically, together with the state equations. An alternative approach is to avoid the use of ϕ and to directly integrate a matrix Riccati differential equation in P (Refs. 9, 10). Such a direct numerical integration provides a mathematically rigorous solution and is readily applicable in the presence of all types of disturbing forces. The method, however,

necessitates the simultaneous integration of a large set of differential equations, thus making the procedure time consuming. As SORKA is designed for real-time operations, it was therefore decided to compute the state-transition matrix in some approximative analytical way. It is realized that this approach may entail subtle but important effects which impair the accuracy of the results, in particular when the analytical expressions for the computation of ϕ require a simplification of the force field while for the state integration a more-extensive force field is used (Ref. 13). At the moment, two alternative analytical techniques have been explored. Experience will show which technique has to be used under specified conditions.

The first method can only be applied if the period between successive measurements is relatively short. It is based on the assumption that the orbit is only affected by earth gravitational forces, and that the expressions for the gradient of the geopotential can be linearized over the time interval between successive measurements. Then, from Eq.(4) the approximative relation

$$\dot{\phi}_{1,0} = M_0 \, \phi_{1,0} \tag{5}$$

can be derived (Ref. 14), where the matrix M_0 can be partitioned into four sub-matrices: two being a 3x3 null matrix, one a 3x3 unit matrix and one a 3x3 matrix containing the second-order partial derivatives of U with respect to the X, Y and Z components of the state vector. Integration of Eq.(5) leads to an exponential function which can be approximated by the series expansion:

$$\phi_{1,0} = I + M_0 \, \Delta t + \tfrac{1}{2}(M_0 \, \Delta t)^2 + \tfrac{1}{6}(M_0 \, \Delta t)^3 + \ldots$$

where $\Delta t = t_1 - t_0$. Analytical expressions have been derived for the second-order derivatives of the geopotential where the effects of the zonal harmonics J_2 upto J_6 and the first tesseral harmonic $J_{2,2}$ were accounted for. These expressions, as well as the expressions for

the first-order partial derivatives which are required for the state integration, were composed by applying the REDUCE formula-manipulation computer program, which is available on the DEC-10 computer of Twente University of Technology. Though this analytical technique of computing ϕ has been implemented in SORKA and has been tested extensively, for the computations described in this report a second analytical technique has been used exclusively.

This second technique was developed primarily for the computation of the state-transition matrix for longer periods between two successive measurements, such as between two different passes. In this technique, the analytical expressions for the elements of the state-transition matrix were obtained by applying the chain-rule to the relations that exist between the state vector and the orbital elements at any time, and to the relations between the orbital elements at a time t_1 and those at t_0:

$$\frac{\partial \underline{X}_1}{\partial \underline{X}_0} = \left(\frac{\partial \underline{X}}{\partial \underline{p}^{osc}}\right)_1 \cdot \frac{\partial \underline{p}_1^{osc}}{\partial \underline{p}_0^{osc}} \cdot \left(\frac{\partial \underline{p}^{osc}}{\partial \underline{X}}\right)_0$$

where $\underline{p}^{osc}$ denotes the vector of osculating orbital elements. The matrices in brackets can be derived easily from the geometrical expressions describing a Keplerian orbit relative to the non-rotating geocentric reference frame (e.g. Ref. 15). To avoid the classical problems for orbits with very low eccentricity or inclination, in principle the use of non-singular orbital elements is preferable. It was demonstrated in Ref. 16, however, that in practice, if the computations are performed on a computer with a reasonable word-length, the problems occur only at extremely low values of eccentricity or inclination. For a word-length of 64 bits, for example, the classical elements can be used if e and sin(i) are larger than 10^{-10}. For simplicity, therefore the classical elements were adopted in SORKA to compute the state-transition matrix. To guarantee that singularity problems will never occur, a simple engineering measure can be introduced which precludes

that e and sin(i) can take values smaller than 10^{-10}.

It has been shown in Ref. 16 that, for the application described in this report, the matrix $\partial \underline{p}_1^{osc}/\partial \underline{p}_0^{osc}$ can be computed with sufficient accuracy by neglecting short-periodic and long-periodic perturbations in the osculating elements, and by taking into account only the secular perturbations due to the oblateness of the earth (J_2). If the orbital altitude is less than 400 km, which is very unlikely for geodetic satellites, also the secular perturbations due to atmospheric drag should be accounted for. Analytical expressions were derived to compute the matrix when only these two types of perturbations are considered. In SORKA only the J_2 secular perturbations are taken into account when the state-transition matrix is computed in this way. The computation sequence is as follows. From the state estimate at the start of the filter process, the osculating elements are computed. These are converted into "mean" orbital elements by subtracting the short-periodic J_2 perturbations, according to the non-singular elements conversion technique described in Ref. 17. The values of the orbital elements at the start of a pass, t_0, are computed by assuming that the elements show only a secular variation (e.g. Ref. 18). Then, the quantities $\partial \underline{p}_0/\partial \underline{X}_0$ are computed, applying the usual transformation relations between (osculating) orbital elements and position and velocity. Subsequently, the quantities $\partial \underline{p}_1/\partial \underline{p}_0$ and $\partial \underline{X}_1/\partial \underline{p}_1$ are computed. Finally, the quantities $\partial \underline{X}_1/\partial \underline{X}_0$ can be evaluated. It is realized that the accuracy of this technique is questionable. In particular, the assumptions that the "mean" elements vary approximately linear with time, and that in the geometrical relations between the rectangular state components and the orbital elements, the "mean" elements can be substituted, may introduce serious errors. This will be investigated in a follow-on study.

As an example of the actual variations of $\partial \underline{X}/\partial \underline{X}_0$, Fig. 2 shows the behavior of two elements over one orbital revolution starting at one day after t_0. The plots refer to a near-circular orbit at an altitude of

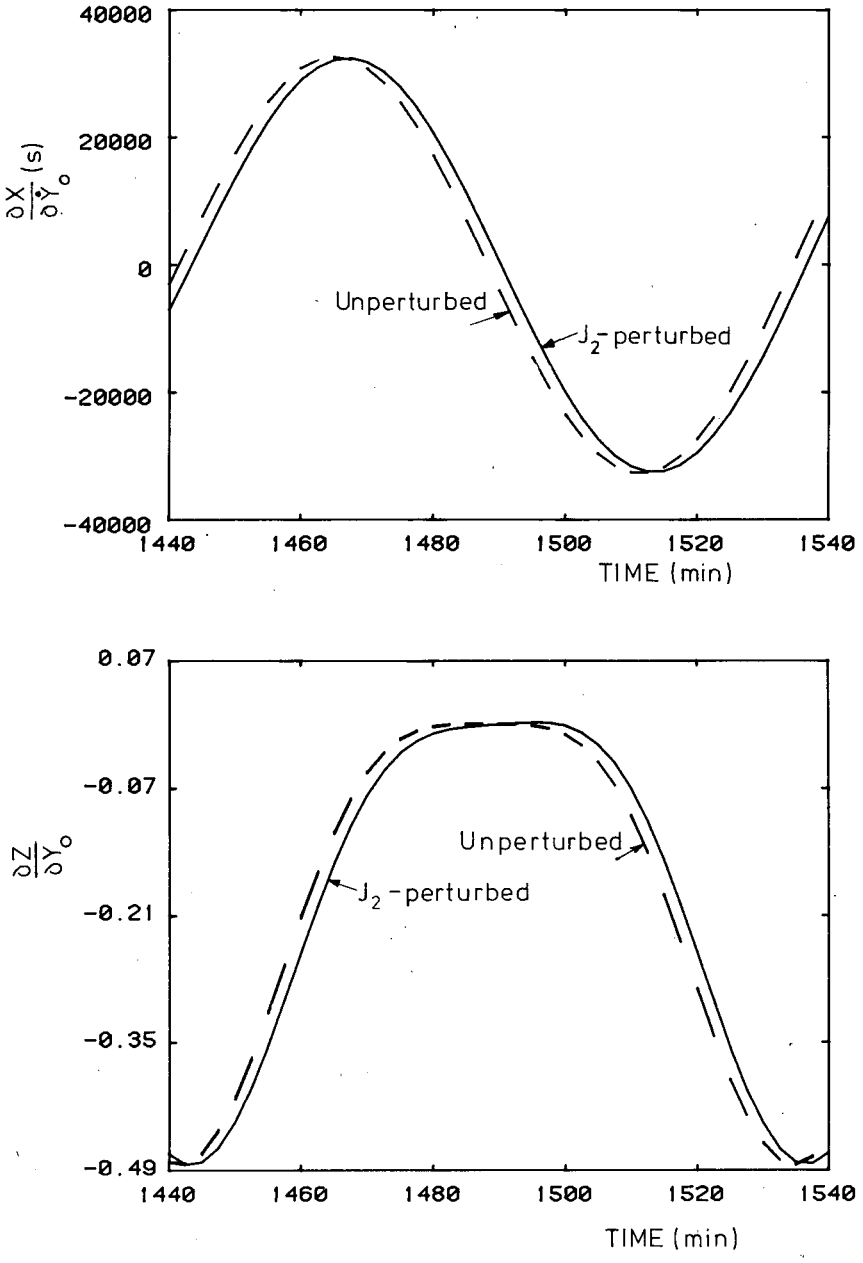

Fig. 2: The effects of J_2-perturbations on the variation of two elements of the state-transition matrix over one orbital period.

425 km and an inclination of 97^{o}. The dashed lines represent the unperturbed variations. When the atmospheric drag perturbations were included, the variations on this scale completely coincided with the dashed line, clearly indicating that contributions due to atmospheric drag are negligible for this period. The solid line holds for the J_2 perturbations, which are shown to have a small but discernable effect.

5. The state-noise covariance matrix

It is well known that Kalman filter applications often suffer from state estimate divergence problems. In principal, these are a result of non-linearities, errors due to an incomplete mathematical model and to a lesser extend also of computational truncation and round-off errors. Physically, the state divergence can be explained as follows. When during the observations processing the state estimates become more accurate, and hence the covariance matrix becomes smaller, the Kalman gain matrix will decrease. As a result, new observations, which reflect the true state, have a smaller effect on the solution than the previous observations. If there is any error in the dynamical model that is not accounted for properly by the assumed model errors, represented by the state-noise covariance matrix Q, then successive estimates of the state may tend to follow the erroneous "learned" dynamical model and to diverge from the true state. Consequently, the estimated state covariance matrix fails to represent the true estimation error.

In the time-update step the state vector and its covariance matrix are integrated. During this integration, errors will be introduced due to dynamic modeling errors and integration errors. Generally, the errors will be non-random. Methods have been developed (e.g. Ref. 8, 9, 11, 19) to account for the model errors in some way. For computational simplicity, in SORKA the crude assumption has been made that the errors are random and can be handled by a proper choice of the covariance matrix Q. A suitable choice for Q that prevents filter divergence has to come from experience gathered during a sufficient number of tests on the filter performance. In SORKA, two methods are used to

compute the state-noise covariance matrix.

For the short time intervals between successive laser observations during a pass, the computation is based on the assumption that the unmodeled forces acting on the satellite yield accelerations that have the same root-mean-square value in all three coordinate directions. At the moment, a value of 10 m/s/day has been selected. From these accelerations, the standard deviations of the velocity errors after a time-update step can be found by simply multiplying the acceleration by the length of the time interval. These three standard deviations of the velocity are the only components of Q that are used. The standard deviations of the position error after the next time-update step evolve from these components through the state-transition matrix. Though this assumption looks questionable, it was found that this method gives realistic results. The along-track position error standard deviation shows the well-known secular trend, while the behavior of the standard deviations in the other two components corresponds to a sinusoidal behavior of these components.

For the integration interval between successive passes, the computation of Q is done in another way. Fixed values are chosen for the along-track, cross-track and radial position errors and for the corresponding velocity errors, which are assumed to be a specified fraction of the position errors. The values selected are 400 m and 0.4 m/s for the cross-track and radial position and velocity components, and 200 m/day and 0.2 m/s/day for the along-track components. So, the along-track components depend on the length of the time interval between the passes and show the well-known secular trend. A few dominant correlations are also introduced in the state-noise covariance matrix in cross-track, radial and along-track components. Finally, an orthogonal transformation is applied to obtain the corresponding matrix in X, Y and Z components. The Q-matrix is then added to the state covariance matrix, P, which has been integrated in one step over the com-

plete time interval between the passes, using the analytically computed state-transition matrix.

6. Behavior of the Kalman gain matrix

The Kalman filter technique has been developed for linear systems. When the filter is applied to orbit dynamics, approximations linearized about a reference state are used. For the filter to work properly, the Kalman gain matrix, being a function of the observation matrix, H, should be nearly independent of the chosen reference state.

From the behavior of the Kalman filter in the observation-update step it was found (Ref. 20) during testruns with simulated data of GEOS-3 (Section 8) that when only range measurements are processed the gain matrix is sometimes strongly dependent on the reference state. To investigate this phenomenon in detail, the predicted state vector and its covariance matrix were extracted out of a Kalman filter simulation run at the time of the fourth observation, when problems first occurred. The state vector and the covariance matrix were used to compute the observation matrix and the Kalman gain matrix, which reduce to a row matrix and a column matrix, respectively, as only range measurements are processed. Then, the state vector was varied systematically in the direction indicated by $K\underline{z}$, as this is the direction in which the state corrections will occur in the observation-update step. For each new state vector, used then as an alternative reference state, new gain matrices were computed. As range-only measurements are used, primarily containing information on the satellite's position, the variation in the position components of the gain matrix was considered to be the most important for the investigation of the phenomenon.

The computations were made for three different measurement standard deviations, σ_{obs}, of 10 m, 1 m and 0.1 m, respectively. As the correlations in the state covariance matrix will have a large effect on the gain matrix, the computations were repeated with slightly smaller values for the correlations. This was simply achieved by multiplying

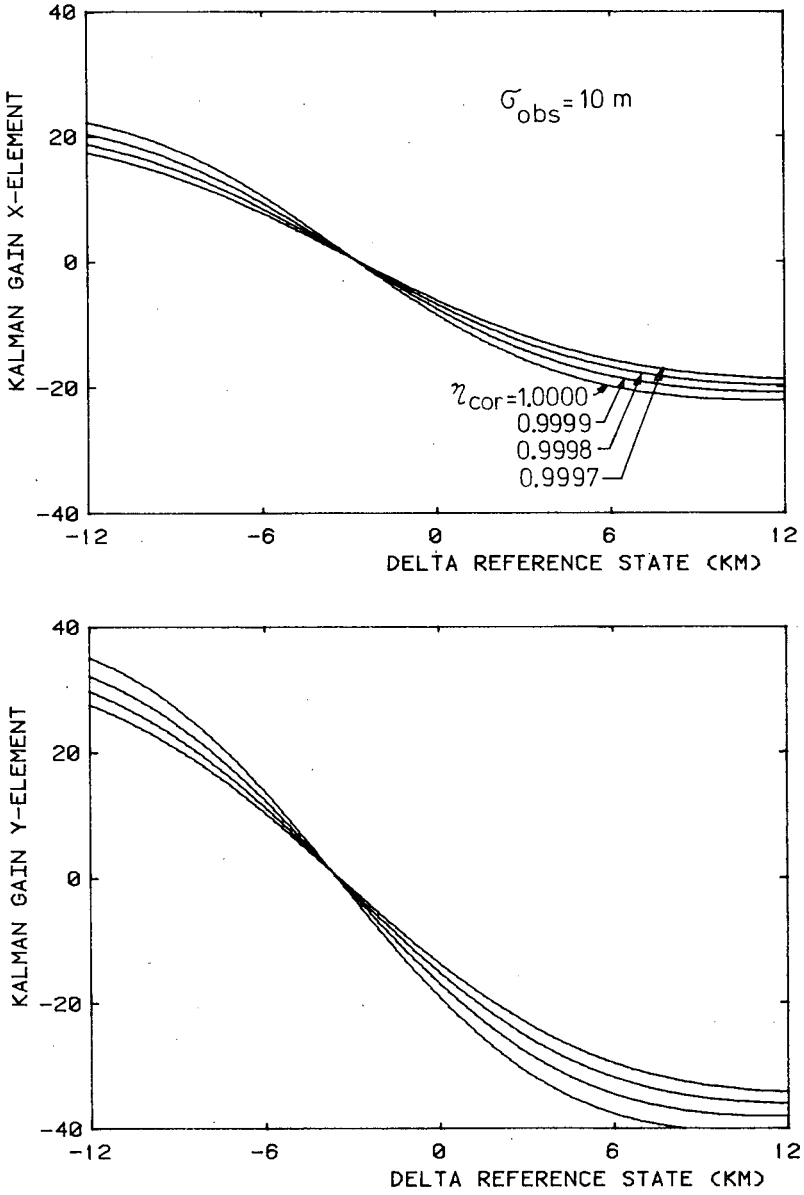

Fig. 3: The dependence of the gain matrix X- and Y-elements on the reference state and the correlations in the state covariance matrix for three different observation standard deviations.

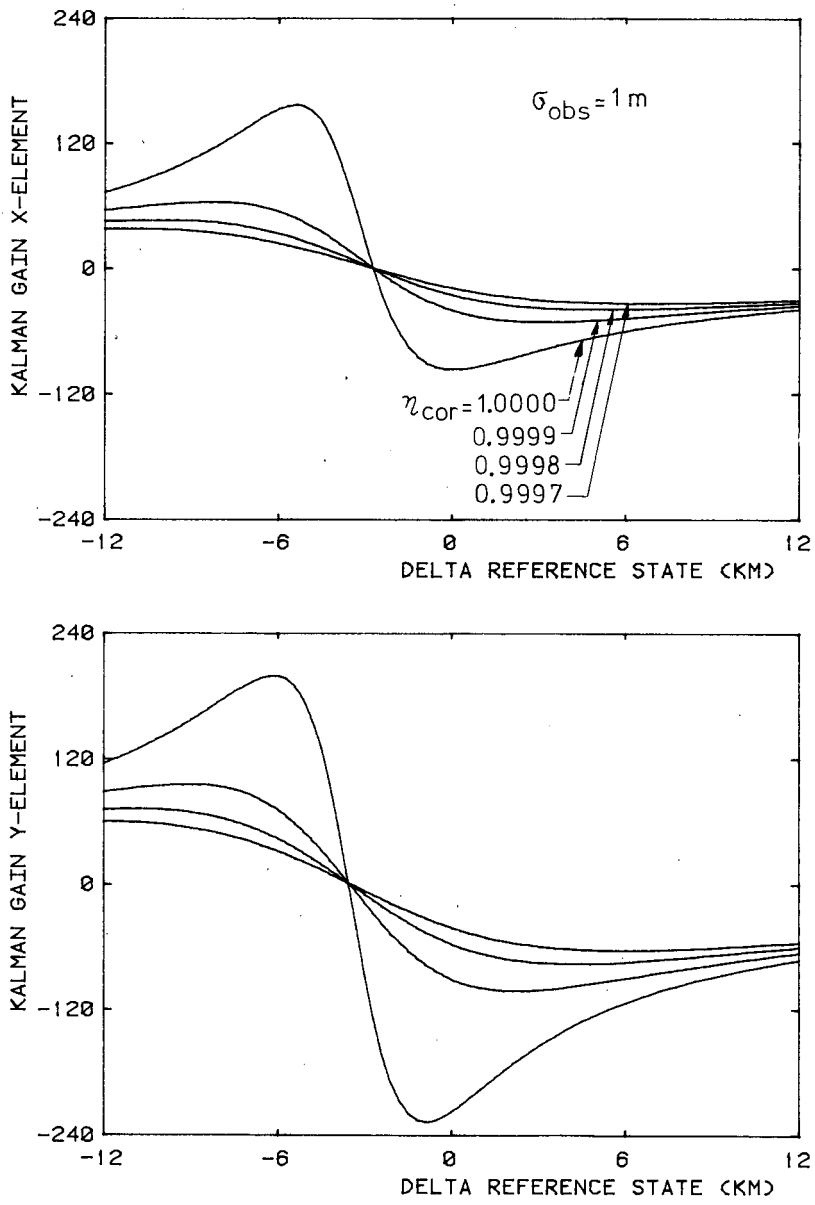
240
120
0
-120
-240
KALMAN GAIN X-ELEMENT
σ_{obs} = 1 m
η_{cor} = 1.0000
0.9999
0.9998
0.9997
-12
-6
0
6
12
DELTA REFERENCE STATE (KM)
240
120
0
-120
-240
KALMAN GAIN Y-ELEMENT
-12
-6
0
6
12
DELTA REFERENCE STATE (KM)

Fig. 3: (Cont.)

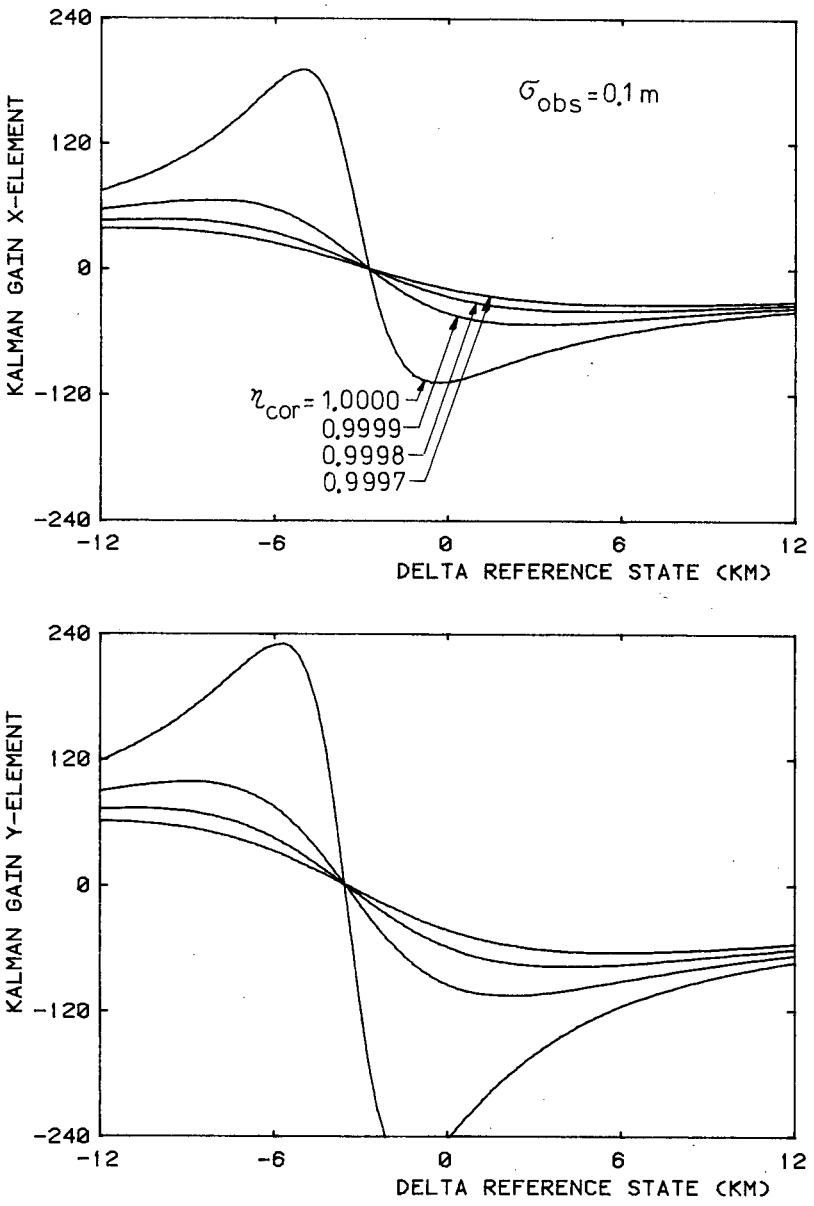
240
120
0
-120
-240
KALMAN GAIN X-ELEMENT
σ_{obs} = 0.1 m
η_{cor} = 1.0000
0.9999
0.9998
0.9997
-12
-6
0
6
12
DELTA REFERENCE STATE (KM)
240
120
0
-120
-240
KALMAN GAIN Y-ELEMENT
-12
-6
0
6
12
DELTA REFERENCE STATE (KM)

Fig. 3: (Cont.)

these numbers by a factor η_{cor} of 0.9999, 0.9998 and 0.9997, respectively. The computed results for the elements of the gain matrix that affect the X- and Y-components of the state vector are shown in Fig. 3. For the Z-component similar results were obtained. The plots clearly show that for a measurement accuracy of 10 m, only a slight dependency of the gain on the reference state exists, while the correlations also hardly affect the results. For measurement accuracies of 1 m and 0.1 m, which are commonly met in laser ranging, the behavior of the gain matrix, however, shows a nearly-singular trend. Relatively small changes in the reference state may lead to large changes in the gain matrix and hence to large variations in the state correction. The plots also show that the reduction of the correlations has a smoothing effect on the gain in the region where near-singularity occurs.

The high correlations are almost unavoidable when processing highly-accurate laser range data, in particular at the start of a pass. They are caused by the use of a fast sequence of very-accurate observations. Because of the short time interval, the different observations are almost in the same direction, thus containing almost identical information. As the observations give no direct information on the velocity of the satellite, the state covariance matrix will inevitably contain high correlations. In Ref. 20 a geometrical explanation of the gain behavior is given and an iteration scheme in the observation-update step is proposed to find a reference state that yields better filter performance than the reference state $\underline{X}_1$, usually applied to compute the observation matrix, H. In the first iteration step, the initial state estimate $\underline{X}_1$ is used as the reference state. In subsequent iterations the mean of the updated estimate $\hat{\underline{X}}_1$ and the initial estimate $\underline{X}_1$ is used for the reference state. This process stops if the computed values for the reference state have converged. During the iterations the matrix P_1 and the residuals, $\underline{z}_1$, are held fixed, while at each iteration new values of H_1, K_1, $\hat{\underline{X}}_1$ and $\hat{P}_1$ are obtained.

Although this iteration scheme improved the stability of the filter, the high values of the gain matrix still occurred and sometimes the iteration scheme did not converge. The basic reason for this is that the iteration scheme results in a reference state that still may not be the "real optimum" for the Kalman filter. So, errors can still be present in the state estimate and these errors are not accounted for in the linear Kalman filter theory. Especially in the near-singularity region, these errors can be very large. To reduce the errors, the dependency of the Kalman gain matrix on the reference state should be reduced. This reduction can be achieved by changing the measurement covariance matrix or by changing the state covariance matrix, as is clearly indicated in Fig. 3.

The selection of larger values for the standard deviations of the observations must be done very carefully as it also affects the gain matrix when singularity is not a problem. Then, it will lead to pessimistic state estimates. A more selective and more powerful method is to modify the correlations in the state covariance matrix. As can be seen in Fig. 3, a small decrease of the correlations by 0.01 percent has a tremendous effect on the gain matrix in the near-singularity region. Outside this region, the gain matrix remains almost unchanged. It proved that this modification of the correlations is a most efficient way to stabilize the filter, and, in the testcases investigated, more effective than the iteration process.

In SORKA, both methods are applied. Before each observation-update step, the correlations in the state covariance matrix are implicitely decreased by multiplying the diagonal terms by a factor slightly greater than one (by default 1.0001). If, occasionally, the iteration process in the observation-update step does not converge, a combination of applying the correction factor and larger observation standard deviations is used to try to achieve convergence. If convergence still cannot be achieved the observation is rejected.

7. Divergence detection

A proper use of the techniques described in the previous Sections will in general lead to a stable Kalman filter behavior when processing laser range observations. In this context, it should be realized that the effect of accounting for the model errors by the matrix Q, discussed in Section 5, is principally different from the effect of the correction factor η_{cor}, described in Section 6. The first one increases the state covariance matrix resulting in larger state corrections during the observation-update step. The factor η_{cor} decreases the gain matrix, resulting in smaller state corrections and larger state covariance matrices. Thus, both methods result in larger covariance matrices, but the first method increases the state vector corrections, while the second method decreases the corrections. Both features can be used to tune the filter process, depending on the number and type of observations, the characteristics of the orbit, etc. Nevertheless, sometimes divergence of the filter occurs, which results in incorrect and useless state vector estimates. In simulations, divergence can be detected very easily. In those cases, divergence is recognized if the estimated state vectors deviate considerably more from the simulated state vector, from which the simulated observations are computed, than the estimated state vector standard deviations given by the state covariance matrix. If real observations are processed, such a comparison, of course, is not possible.

The only way to detect divergence in real observations processing is to study the observation residuals, $\underline{z}$. The observation residuals relative to the predicted state vector at the time of an observation are used in the observation-update step. The covariance matrix of the residual vector, i.e. $R + HPH^T$, is used in the computation of the Kalman gain matrix. Thus, for divergence detection there is available a sample of a stochastic variable (the residual vector), which in the Kalman filter is assumed to have a Gaussian distribution with zero mean and known covariance matrix, and which is assumed not to be correlated in time. Methods can be developed to test the validity of one or a combination of these assumptions.

The two divergence detection methods implemented in SORKA are based on testing the validity of the residual covariance matrix. Therefore, the squared residual is weighted with the covariance matrix. This squared weighted residual is a stochastic variable which should have a chi-squared distribution, with, in case of range-only measurements, one degree of freedom per observation. The sum of these variables can be used to test, with a given degree of confidence, if the variables indeed correspond with their distribution. However, as after a number of processed observations this method will become very slow, in SORKA two faster divergence detection techniques are included. One method is based on a fading-memory filter, in which the most recent residuals have a greater weight in the sum. The other is based on the low-pass filter technique described in Ref. 21, which also results in a test which is more sensitive to the last measurements. The two methods are at present not fully tested, and no definite preference for one of them exists. Both methods are handicapped if only a few observations during a pass are available, but were found to work satisfactory if many observations are processed.

8. Results

To investigate the general behavior of SORKA when processing laser range observations from only one groundstation many simulations were performed. In these tests simulated observations of GEOS-3 (Table 1) were processed. The first results of these simulations are reported in Refs. 22, 23; the final results are discussed in Ref. 20. In these final simulations, four passes of GEOS-3 over Kootwijk were selected, for which also corresponding real observations were available. These passes took place within a 30-hour period on November 27, 1977. For the simulations, an initial state vector was chosen which led to an orbit that closely resembled the real orbit of GEOS-3 at that time. From an accurate numerical integration simulated state vectors and simulated observations were computed with an interval of 12 s between successive observations during a pass. All observations that were not

Table 1: Satellite data

	GEOS-1	GEOS-3
Satellite number	6508901	7502701
Launch date	Nov. 6	April 9
Shape	octagonal prism with hemispherical cap on down end and octagonal pyramid on top	octagonal prism with radar altimeter dish on down end and octagonal pyramid on top
Dimensions (cm)	132 wide 81 high	132 wide 81 high
Mass (kg)	172.5	345.9
Stabilization	gravity-gradient	gravity-gradient
Transmitters	TRANSIT and MINI-TRACK beacon. SECOR and GRARR transponders	doppler beacon. C-band and S-band transponders. Radar altimeter.
Laser reflectors	322 reflectors on 0.18 m^2 bottom-mounted flat array	264 reflectors in conical ring around the periphery of bottom side
Orbit*		
a (km)	8073	7221
e	0.0717	0.0014
i (deg)	59.4	115.0
P (min)	120	102

*Mean elements for mid 1978.

present in the real data were removed. These simulated observations were then contaminated with noise of 1 m standard deviation. The initial state estimate was also contaminated with noise of 1 km standard deviation in the position components and of 1 m/s in the velocity components. To summarize the results, it can be stated that SORKA proved to be able to yield acceptable state estimates. It was found that the effects of applying the correction factor η_{cor}, des-

cribed in Section 6, were very significant: a simulation without the correction factor diverged immediately after the fourth observation. Changing the values for the root-mean-square of the unmodeled accelerations from 10 m/s/day to zero, or by-passing the iteration scheme in the observation-update step, showed to have much smaller effects in these tests. A few simulations with slightly different values for the initial state vector, however, demonstrated that the errors in the state estimates, and the effects of the various stabilizing features incorporated in SORKA, are heavily dependent on the accuracy of the initial state.

The first experiences with SORKA in processing real range observations look also very promising. Another set of measurements was selected. These measurements were acquired at Kootwijk during 8 passes of GEOS-1 (Table 1) in the period July 11 to July 13, 1978. The data-arc with a length of 54 hour comprised 611 measurements. During this period the satellite completed 27 revolutions. These observations were also used in studies, described in Refs. 24, 25 to estimate from laser range data acquired at Kootwijk and Wettzell (Fed. Rep. Germany) the coordinates of the Wettzell laser station. In those studies the orbit was determined using the least-squares batch-processing GEODYN computer program (Ref. 26). Because of the very high accuracies obtainable with GEODYN, that solution for the orbit could serve as the reference to which the SORKA results are compared. The initial state was taken to be the state estimated by GEODYN; the initial standard deviations for the radial, cross-track and along-track position and velocity components were assumed to be 1 m and 0.03 m/s, respectively. So, this experiment reflects the (hypothetical) situation of extremely accurate initial state estimates. The standard deviation of the observations was taken to be 0.25 m, which is about the actual accuracy of the Kootwijk laser system.

In Fig. 4 the sub-satellite points at the times of the observations

Fig. 4: The GEOS-1 sub-satellite points at the observation times. The general direction of the satellite motion is from west to east.

are plotted. The range residuals for all eight passes are shown in Fig. 5. The results for the different passes are plotted one after another, neglecting the different periods between the passes. From this Figure, it can be concluded that the Kalman filter showed a satisfactory stable behavior for all passes. For more-detailed information on the performance of the filter, in Fig. 6 the differences between the state components as computed by SORKA and the values computed by GEODYN are depicted for the first two passes over Kootwijk. These differences, which are considered as the Kalman estimate errors, are given in terms of cross-track, radial and along-track errors. The solid lines indicate the standard deviations of the state estimates, as provided by the Kalman filter. The Figure shows that the errors in the position components are generally less than 100 m, with the largest errors occurring in the cross-track component. This result could be

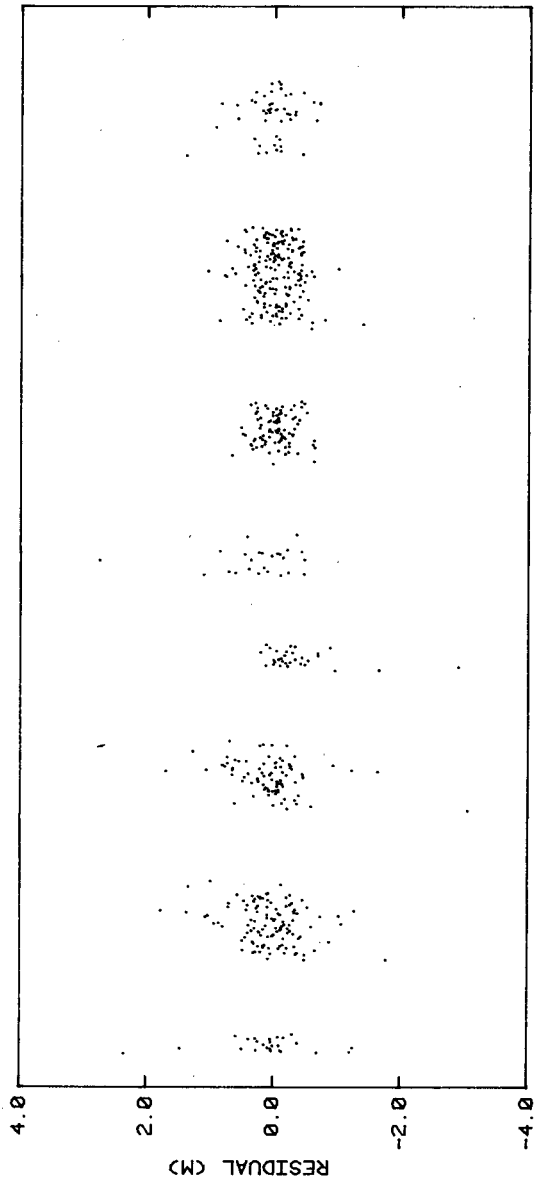

Fig. 5: The range residuals for the eight GEOS-1 passes over Kootwijk

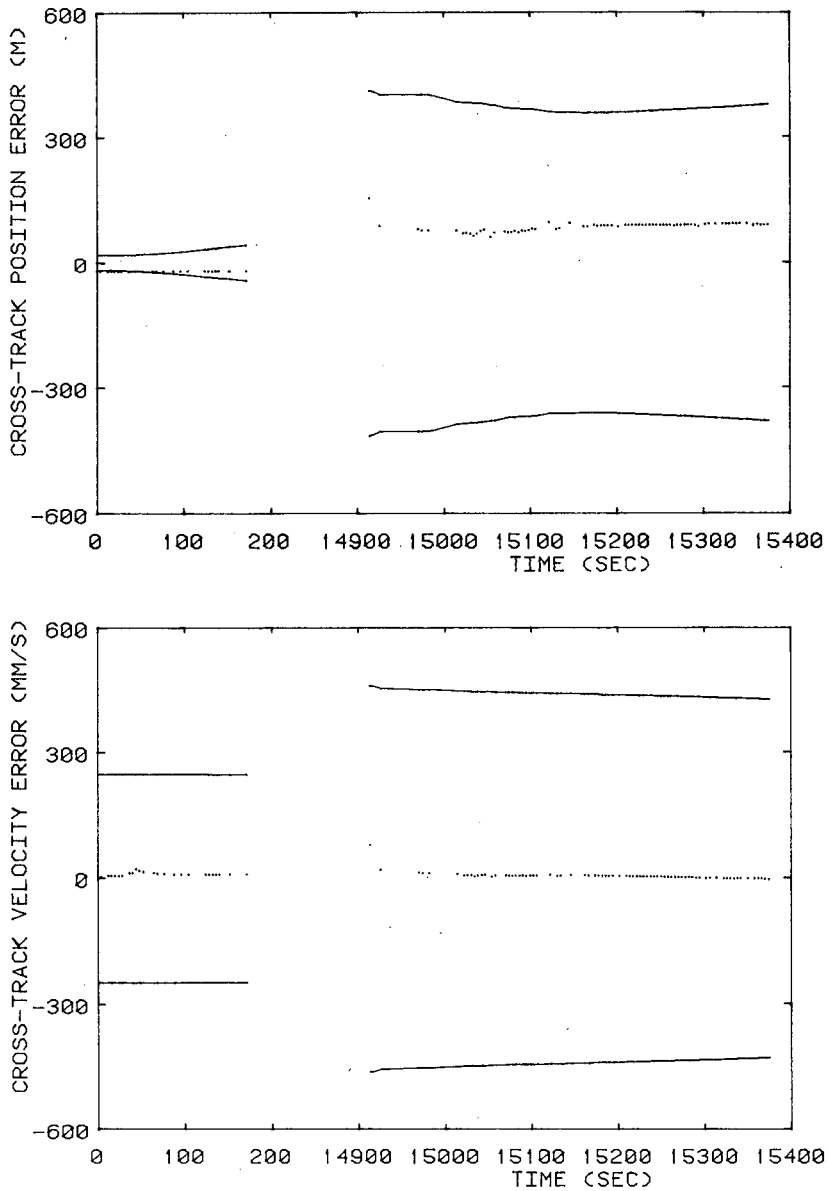

Fig. 6: The actual errors in the state components and the estimated standard deviations for the first two passes of GEOS-1 over Kootwijk.

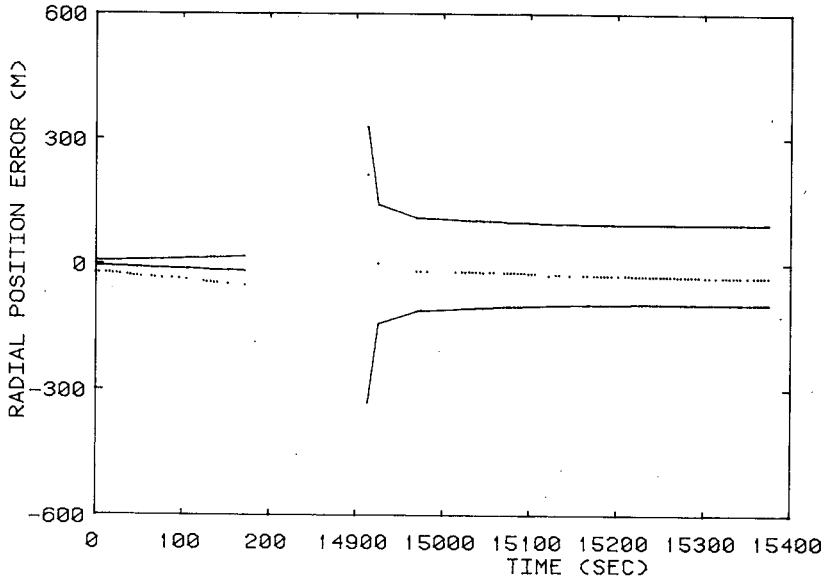
600
300
0
-300
-600
RADIAL POSITION ERROR (M)
0
100
200
14900
15000
15100
15200
15300
15400
TIME (SEC)

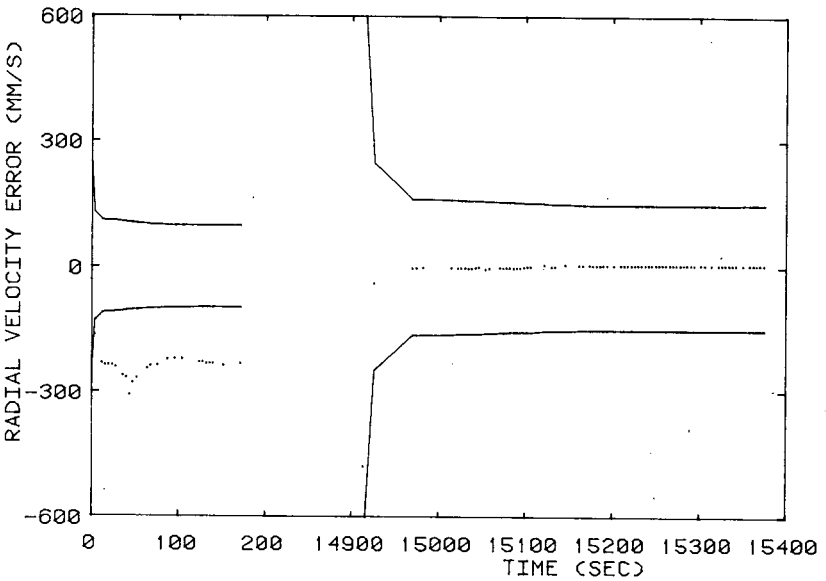
600
300
0
-300
-600
RADIAL VELOCITY ERROR (MM/S)
0
100
200
14900
15000
15100
15200
15300
15400
TIME (SEC)

Fig. 6: (Cont.)

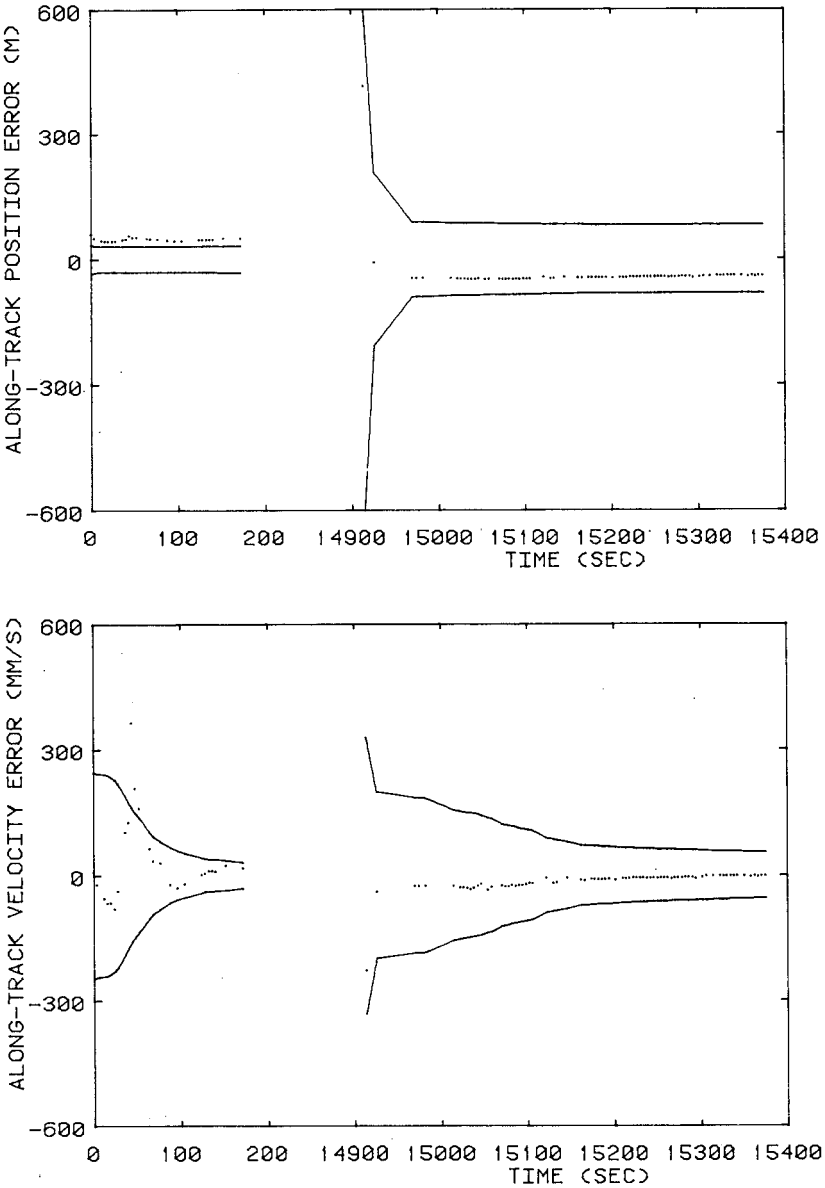
ALONG-TRACK POSITION ERROR (M)
600
300
0
-300
-600
0
100
200
14900
15000
15100
15200
15300
15400
TIME (SEC)
ALONG-TRACK VELOCITY ERROR (MM/S)
600
300
0
-300
-600
0
100
200
14900
15000
15100
15200
15300
15400
TIME (SEC)

Fig. 6: (Cont.)

expected because range observations from a single or a few passes contain almost no information on the orientation of the orbital plane. Consequently, cross-track errors are not filtered out easily. At the very beginning of the second pass larger position errors of up to 1 km are encountered. As soon as new observations are processed, these errors decrease very fast. The estimated accuracy of the position components shows up to be rather conservative, in particular during the second pass. The errors in the velocity components during the first pass are less than 0.3 m/s, with the largest errors occurring in the radial and along-track components. At the start of the second pass errors of up to 0.8 m/s are found. Again, these errors decrease very fast as new observations are processed to generally less than 0.03 m/s. Also for the velocity components the accuracy estimation yields conservative values. As for the estimated position errors these are probably due to over-pessimistic model accuracy estimates.

The total position and velocity errors for the whole period are depicted in Fig. 7. To show both the short-term behavior and the increase of the errors and the estimated standard deviations during the 40-hour period between the third and the fourth pass, a logarithmic scale (to the base 10) has been applied. State errors are plotted at 20-minute intervals. It is clearly visible that during the 40-hour period in which no observations are available the position error increased to about 14 km, and the velocity error to 12 m/s. As soon as the first observations of the fourth pass have been processed, the errors immediately decrease to the level of the first passes.

In this numerical experiment, actual observations were processed. It will be evident that when SORKA, in its current version, would have been used to point the laser at the satellite, some searching process would have been necessary in order to acquire the first observations during a pass. For instance, assuming that the distance of GEOS-1 to the laser at the start of the fourth pass is 2500 km, the position error of 14 km corresponds, depending of the pass geometry, to a topo-

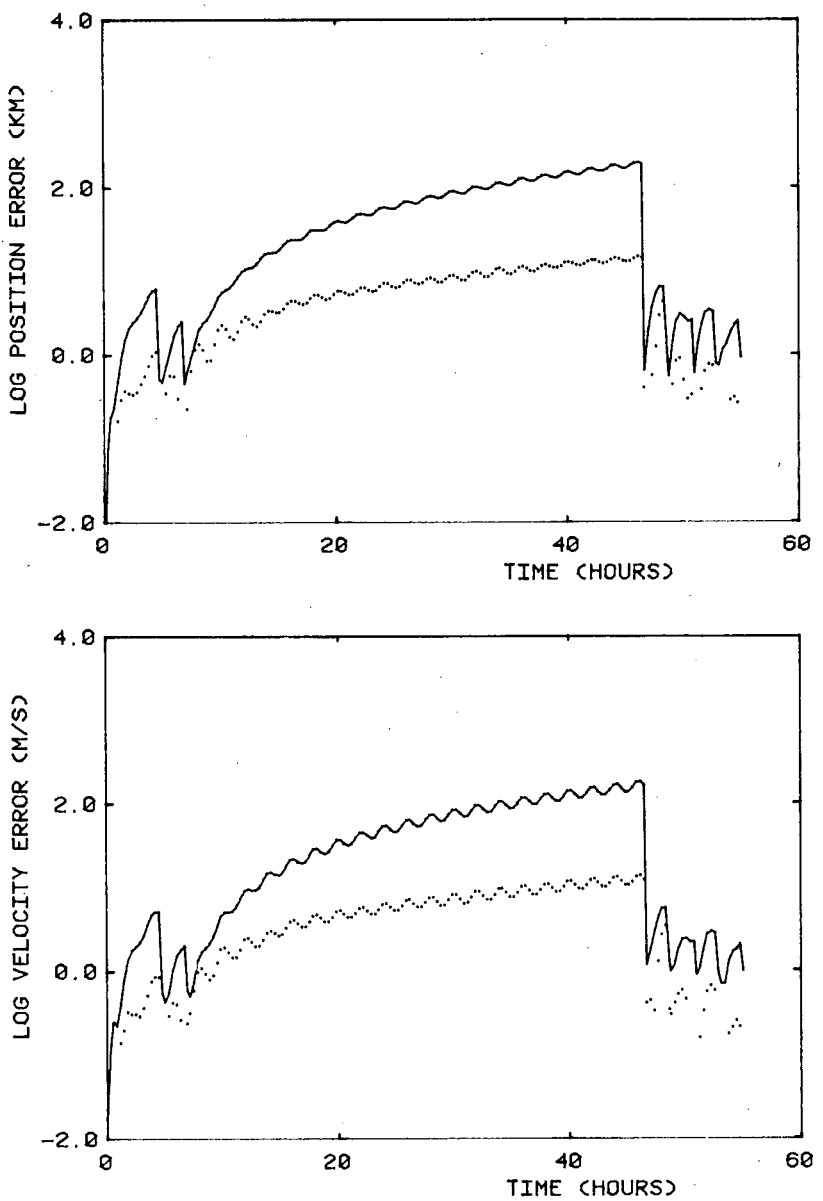

Fig. 7: The long-term behavior of the actual total position and velocity errors and the estimated standard deviations.

centric angular error of 10' to 20', or about the same magnitude as the maximum beam divergence of the Kootwijk laser. Because, usually, much narrower beams are applied, a systematic search would have to be performed to acquire the first returns. Even if smaller position errors can be obtained with future versions of SORKA, such searching procedures might still remain necessary. Which procedure will be selected has not yet been determined.

9. Conclusions and prospects

For investigating the possibilities to use laser range observations acquired at the Kootwijk satellite observatory for (semi-) real-time improvement of the predicted satellite positions, a computer program called SORKA has been developed. The main requirements were that SORKA could satisfy both the accuracy level needed for the laser to hit the satellite and the capabilities of a small local computer. Until now, SORKA runs on an IBM 370/158 computer and the implementation on a local computer still has to be studied. In the design of SORKA precautions have been taken to make such an implementation possible.

The first tests in applying SORKA to simulated and real observations look promising and justify the continuation of the efforts to improve the computations scheme such that the laser pointing capabilities are optimized. It has been demonstrated that a stable Kalman filter process can be obtained when using only laser range measurements from one ground-station. It was found that divergence, which very easily may occur due to high correlations in the state covariance matrix, which in turn are a direct result of processing only laser range measurements, could effectively be suppressed by applying a correlation correction factor and an iteration scheme in the observation-update step.

The study has revealed specific shortcomings of the current SORKA program and has indicated directions to improve the program's capabilities. Only a few of these future improvements will be mentioned

below.

To decrease the errors in the predicted state after a period between two successive passes, both the state estimate at the end of the preceeding pass and the mathematical model describing the motion during that intermediate period have to be improved. To increase the accuracy of the state estimate at the end of a pass a global iteration scheme will be introduced where the final state vector is integrated backwards over a few passes. The number of passes has to be selected such that sufficient information will be gained on the orientation of the orbital plane. Then the observations are processed again. For the period in between two successive passes, which period may last for many hours, as well as for the second and higher steps in the global iteration, a more-extensive dynamical model will be used.
Both changes do not affect the real-time performances of the program as the computations are performed during the idle periods between the passes. Furthermore, the various parameters which are used to tune the filter process will be optimized to yield the most accurate results, and one of the divergence detection methods will be linked in a closed-loop mode to correct for divergence as soon as such a tendency is detected.

As mentioned in Section 2, it may be attractive to use the laser pointing angles during the search process as observations. Although the accuracy of these observations is very low in comparison with the range measurements it will be investigated if the inclusion of these angles will have a stabilizing effect on the filter. Also, it will be investigated if non-linear filtering techniques (e.g. Ref. 27) will offer practical advantages over the currently applied extended Kalman filter.

10. References

1. Aardoom, L. and Zeeman, F.W., The satellite ranging system at Kootwijk, in: Proceedings of Laser Workshop, National Technical University, Athens, 1978, pp. 89-96.
2. Aardoom, L., Kootwijk SLR station status, paper presented at the third LAGEOS Working Group Meeting, NASA Goddard Space Flight Center, October 1980.
3. Ambrosius, B.A.C., Piersma, H.J.D. and Wakker, K.F., Description of the AIMLASER satellite orbit prediction program and its implementation on the Delft University IBM computer, Report LR-218, Delft Univ. Technology, Dept. Aerospace Engin., 1976.
4. de Groot, W.A., Investigation on the accuracy of the SAO orbital elements (in Dutch), Delft Univ. Technology, Dept. Aerospace Engin., 1978.
5. Jazwinski, A.H., Stochastic processes and filtering theory, Academic Press, New York, 1970, pp. 272-281.
6. Williams, D.E., A geometric derivation of the Kalman filter equations, Technical Report 78122, Royal Aircraft Establishment, Farnborough, 1978.
7. Rogers, C.E. and Christodoulou, C., The extended Kalman filter applied to the determination of the orbital parameters of a passive earth satellite, Thesis Air Force Institute of Technology, Wright-Patterson AFB, 1971.
8. Tapley, B.D. and Schutz, B.E., A comparison of orbit determination methods for geodetic satellites, Proc. of First International Symposium on the Use of Artificial Satellites for Geodesy and Geodynamics, Athens, 1973, pp. 523-562.
9. Tapley, B.D., Statistical orbit determination theory, in: Recent advances in dynamical astronomy, Reidel, Dordrecht, 1973, pp. 396-425.
10. Schutz, B.E., McMillan, J.D. and Tapley, B.D., A comparison of estimation methods for the reduction of laser observations of a near-earth satellite, AAS/AIAA Astrodynamics Conference, Vail, 1973.
11. Torroglosa, V., Filtering theory applied to orbit determination,

ESRO CR(P)-532, ESA, Paris, 1973.

12. Thornton, C.L. and Bierman, G.J., A numerical comparison of discrete Kalman filtering algorithms: An orbit determination case study, IAF-76-015, 27th IAF Congress, Anaheim, 1976.
13. Rice, D.R., An investigation into the effects of using simplified force models in the computation of state transition matrices, AIAA Paper No. 67-123, New York, 1967.
14. van Hulzen, J.J.P., Preliminary study on the application of a Kalman filter to the orbit determination of satellites (in Dutch), Delft Univ. of Technology, Dept. Aerospace Engin., 1978.
15. Cornelisse, J.W., Schöyer, H.F.R. and Wakker, K.F., Rocket propulsion and spaceflight dynamics, Pitman, London, 1979, pp. 379-383.
16. Kamp, A., Analytical partial derivatives for a perturbed Keplerian orbit (in Dutch), Technical thesis, Delft Univ. of Technology, Dept. Aerospace Engin., 1979.
17. Merson, R.H., The dynamical model of PROP, a computer program for the refinement of the orbital parameters of an earth satellite, Technical Report 66255, Royal Aircraft Establishment, Farnborough, 1966.
18. Kozai, Y., The motion of a close earth satellite, The Astronomical Journal, 64, no. 1274, pp. 367-377, 1959.
19. Wright, J.R., Sequential orbit determination with auto-correlated gravity modeling errors, Paper AIAA-80-0239, Pasadena, 1980.
20. van Hulzen, J.J.P., Kalman filter satellite orbit determination using laser range observations by a single station, Thesis advanced study, Delft Univ. of Technology, Dept. Aerospace Engin., 1980.
21. Traas, C.R., Digital filtering methods, with applications to satellite attitude determination in the presence of modelling errors, Part 1: Theory, NLR-TR-76048C, National Aerospace Laboratory, Amsterdam, 1976.
22. van Hulzen, J.J.P., Kalman filter satellite orbit determination from simulated laser range observations from one groundstation (in Dutch), Technical thesis, Delft Univ. of Technology, Dept. Aerospace Engin., 1979.

23. Kamp, A. and van Hulzen, J.J.P., State transition matrix computations for Kalman filter orbit determination from laser range observations, paper presented at the 30th IAF Congress, Munich, 1979; also: Memorandum M-363, Delft Univ. of Technology, Dept. Aerospace Engin., 1980.
24. Wakker, K.F. and Ambrosius, B.A.C., A study on the determination of the Kootwijk-Wettzell baseline from satellite laser ranging at these stations, paper submitted to the 2nd meeting of the LAGEOS Working Group, Greenbelt, 1980; also: Report LR-295, Delft Univ. of Technology, Dept. Aerospace Engin., 1980.
25. Wakker, K.F. and Ambrosius, B.A.C., Estimation of the Wettzell coordinates from satellite laser ranging at Kootwijk, San Fernando and Wettzell, paper submitted to the EROS plenary meeting, Grasse, 1980; also: Report LR-296, Delft Univ. of Technology, Dept. Aerospace Engin., 1980.
26. Martin, T.V., GEODYN descriptive summary, contract no. NAS 5-22849, Washington Analytical Services Center, Riverdale, 1978.
27. Chiariglione, L. and Corgnier, L.C., Estimation of continuous-time processes with discrete measurements by Hermite polynomial expansions with application to an orbit determination problem, ESA CR(P)-1148, ESA, Paris, 1978.